

## Roll Bonding of Steel Net-Reinforced Aluminium Strips

Mykhailo Stolbchenko<sup>a</sup>, Hanna Makeieva<sup>b\*</sup>, Olexandr Grydin<sup>a</sup>, Yaroslav Frolov<sup>a</sup>, Mirko Schaper<sup>a</sup>

<sup>a</sup>Materials Science Paderborn, Paderborn University, Germany

<sup>b</sup>Metal Forming, National Metallurgical Academy of Ukraine, Ukraine

Received: October 17, 2017; Revised: November 25, 2017; Accepted: December 14, 2017

The present study is dedicated to the experimental determination of strain parameters at rolling of aluminium matrix with inserted wire netting. Two types of stainless steel fabric netting with different orientation to the rolling axis were placed between two aluminium strips and hot rolled. The rolling temperature and reduction were varied to achieve the sound bonding between the matrix layers and steel net. During the study, the following main investigations were made: strain on areas of longitudinal and transverse cross sections of the composite was measured; stretching and ovalization of net wiring and changes in the net cell angles were determined; mechanical properties of composites along the rolling direction were tested. The experiments were summarized by following contradiction: the contact pressure, required for the bonding of aluminium layers, produces extreme tensile strain on the inserted wires, reducing the mechanical properties of the reinforcing net and, consequently, reducing the properties of the entire composite. Strips with diagonally oriented reinforcing net showed the best results in the longitudinal tension tests.

**Keywords:** aluminium matrix, steel net, reinforcing, rolling, delamination, mechanical properties.

### 1. Introduction

The combination of different materials in a single product, known as a composite, usually incorporates the best properties of each material into a single finished product. An example of such a composite is aluminium alloy sheet reinforced with steel netting. The aluminium is lightweight and highly resistant to corrosion whereas the stainless steel netting is strong and ductile. Moreover, such combination probably should elevate the fire-resistance of composite. The properties and characteristics of such compositions, including those obtained in the metal forming processes, are described in<sup>1</sup>. In the United States, Patent<sup>2</sup> claims the methods of producing a metallic material composite which involves assembling at least two stacked matrix layers of relatively low-strength metal and one or more reinforcements in the form of wire or net. This method involves: a) placing a wire-wrapped aluminum sheet between two additional aluminum sheets and rolling it at 400-450 °C; b) hot rolling a wire mesh sheet placed diagonally between the two sheets of aluminium alloy; c) hot rolling a multilayer composite of interwoven alternate matrix layers, meshes of woven stainless steel and aluminium wires; and d) filling mesh cells with aluminium spraying and rolling between the soft matrix sheets. Aside from production methods, the results of mechanical and fatigue tests of obtained composites are also presented in this patent. They show that all composites had an increased fatigue life, especially with a diagonal net-

reinforcement. However, in some experiments, the rolled composites showed a decreased level of strength and ductility in comparison to pure matrix material. Unfortunately from study<sup>2</sup>, the strain parameters of rolling and the contraction of cross-sectional wiring remain unclear. Patent<sup>3</sup> describes the elements of longitudinal steel wire reinforcing technology of an aluminium matrix during rolling. The methodology begins with the formation of half-rounded longitudinal grooves on the aluminium matrix surface. Steel wire is then placed in the grooves of both matrices and rolled flat. The implementation of these methods avoids significant strain in both the matrix and wiring. In our opinion however, this technology lacks an additional pre-bonding operation in grooving matrices. In patent<sup>4</sup> is described another way of reinforcing, which consist compounding and subsequent rolling of transversally grooved aluminium matrix, with longitudinal steel wires. This technology with a small rolling reduction provides higher contact pressure between the matrix and the reinforcement, as well as between the matrix layers. Its drawback however, is the high probability of a porous appearance inside the finished composite. Authors claim that such porosity can be eliminated following further deformation processes. Both technologies described in<sup>3</sup> and<sup>4</sup> require compliance between the wire diameter and diameter of the groove for each material pairing as well as the determination of strain-temperature conditions of process. Numerous tests were devoted to investigating strain-temperature conditions at roll bonding of flat products.

Experiment<sup>5</sup> analyzes the deformation of the longitudinal and transversal net wires within a flat composite after rolling.

\*e-mail: [anna123makeieva@gmail.com](mailto:anna123makeieva@gmail.com)

Results of the experiment show that the wire cross section changes in two ways during rolling: ovalisation (flattening) and stretching. The set of these deformations depends on the position of wire in the composition as well as on the strain parameters during rolling. The appearance of carbon fibre breakages inside the twin-roll cast composite, presented in<sup>6</sup>, also reflect the importance of monitoring strain parameters during the composite's deformation.

The implementation of the energy-saving twin-roll casting technology for aluminium-steel clad strips allows a thin and uniform layer of intermetallic phases on the materials interface of approximately 3  $\mu\text{m}$  thickness with an adhesive strength of over 70 MPa<sup>7</sup> to be obtained. Moreover, a good cold formability of the twin-roll cast and consequently hot rolled clad strip of pure aluminium and austenitic steel is shown in<sup>8</sup>. The results of the research on the roll bonding of two-layer (Al - Al) and a three-layer (Al - steel - Al) compositions are described in<sup>9</sup>. It is shown that the strain rate during rolling has no significant impact on the composite's mechanical properties. The main parameters are: contact pressure, temperature and strain. A minor number of known studies is devoted to casting technologies, in particular twin-roll casting, for manufacturing aluminium matrix composites reinforced with wires and netting and to the evaluation of their properties. Section<sup>10</sup> describes process parameters and upper limitations of wire diameter by twin-roll casting of net-reinforced aluminium strips. At the same time, the contraction of cross-sectional wiring due to the consequent rolling was not observed considerably. The devices for feeding and positioning of the wires inside the composite during the twin-roll casting are described in<sup>11</sup>. Thus, the current level of research shows that strain-temperature parameters of roll bonding in a certain range can increase composite properties without a preliminary grooving. Establishing this range is necessary in understanding how the rolling parameters impact the contraction of reinforcing phase and how they influence the composite's properties.

The purpose of this work is to obtain quantitative data on the contraction of cross-sectional wiring during the roll bonding of net-reinforced aluminium matrix composites. Moreover, the study serves to evaluate the influence of changes in cross-sectional wiring on the composite's tensile strength.

## 2. Experimental

The flat composite consisting of two outer layers of aluminium alloy and a stainless steel net in the core was manufactured by means of roll bonding. The following aluminium alloys in the form of thin strips were used as a matrix material of the composite:

- ENAW-5056 (Al-Mg system) in the annealed condition; the samples' dimensions for the experimental roll bonding ( $h \times b \times l$ ):  $4 \times 36 \times 120$  mm.

- EN AW-6063 (Al-Mg-Si system) in the annealed condition; the samples' dimensions: ( $h \times b \times l$ )  $3 \times 36 \times 120$  mm.

Alloy AW 5056 was chosen as the matrix due to its strain hardening opportunity. Other matrix material is a representative of thermal hardened alloys.

The two types of the 90° fabric wire nets of stainless steel EN 1.4301 were used as a reinforcement material:

- "A" - diameter of the net wire: 0.5 mm; size of square cell  $3 \times 3$  mm;
- "B" - diameter of the net wire: 0.25 mm; size of square cell  $1 \times 1$  mm.

For each of 4 materials pairs, three types of billets, preliminarily fastened in the corners with aluminium rivets and forming so-called composites, were prepared for the subsequent roll bonding (See Fig. 1):

- Type 90 - the net wires oriented along and across the rolling direction.
- Type 45 - the net wires oriented at an angle of 45° (diagonally) to the rolling direction.
- Type 0 - without reinforcing net.

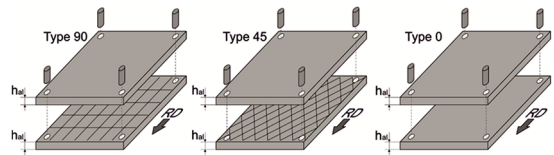


**Figure 1.** Composite preparation scheme for the experiments on roll-bonding: RD - rolling direction,  $h_{al}$  - initial thickness of the aluminium strips.

The rolling was carried out in one or two passes with a nominal reduction of 30% in every pass with a preheating to the rolling temperature (see. Table 1) in a two-high rolling stand with 250 mm diameter rolls. Rolling speed was 23.5 m/min.

The general experimental plan and parameters for the hot roll bonding of aluminium strips reinforced with a steel net is presented in the Table 1.

The only exception in the experimental series was roll-bonding of non-reinforced composites with AW-6063 matrix in one pass. In this case, they were delaminated during machining of specimens, possibly due to an insufficiently high rolling temperature of 200 °C. Further analysis of this composite was impossible. Rolling temperature 500°C was chosen as a common value, widely used in practice. From other hand 200°C and 30% reduction is the lower point of supposed welding possibility on the strain-temperature field.

After the roll bonding, the cross-sections of the manufactured composites in the longitudinal and transversal (to the rolling direction) planes were made to analyze the position and form of the wires in the matrix material. The cross-sections were prepared using abrasive cutoff machine and a subsequent grinding with sandpaper up to 4000 grit.

**Table 1.** The experiments on the hot roll bonding of net-reinforced aluminium composites, where: ● – experiments were performed, – – experiments were not performed.

Features		Matrix alloy	
		AW-5056	AW-6063
Samples	Net type A	●	●
	Net type B	●	●
	Composite type 90	●	●
	Composite type 45	●	●
	Composite type 0	●	●
Processing	Nominal reduction 30% in a single pass, rolling temperature 200 °C	-	●
	Nominal reduction 30% in a single pass, rolling temperature 500 °C	●	-
	Nominal reduction 60%, in two passes with intermediate preheating, rolling temperature 500 °C	-	●
Testing	Measurement of wires strain	●	●
	Quasi-static longitudinal tensile test	●	●

The form and position of the wires in the cross-sections were analyzed and measured using a digital microscope Keyence VHX5000.

To analyze the net distortion of the sample's length and width, one of the matrix layers was removed to reveal the net fabric. For this purpose, one of the aluminium layers was ground and subsequently chemically removed using 5%-solution of NaOH until the net became visible. Photographs of the net inside the composite were taken using digital microscope Keyence VHX5000.

Calculations of strain parameters were carried out as following below. The list of main herewith-used symbols is presented in the Table 2.

Sketches on the Fig. 2 are depicting some important aspects composite's building in initial (Fig. 2a) and after-rolling (Fig. 2b) conditions.

To calculate strain values (Fig. 2a), the initial composite thickness  $h_{0\Sigma}$  was interpreted as the sum of thicknesses of the aluminium matrix  $h_{Al}$  without factoring in the thickness of the netting (1):

**Table 2.** List of main symbols being used at calculations of strain parameters.

Parameter	Description
$i$	subscript; initial (0) or after-rolling (1) condition;
$L$	subscript; projection of the longitudinal wire on the transversal plane;
$T$	subscript; projection of the transversal wire on the longitudinal plane;
90	superscript; composite of Type 90;
45	superscript; composite of Type 45;
$h_{Al}$	thickness of the aluminium matrix;
$h_{\Sigma}$	thickness of the composite;
$b_{\Sigma}$	width of the composite;
$h_{iw}$	measured on the plane height of the wire, initially equals to its diameter;
$b_{iw}$	measured on the plane width of the wire;
$\mu_{\Sigma}$	elongation factor of the whole composite;
$\mu_{iw}$	wire's elongation factor;
$F_{iw}$	cross-sectional area of wire
$\varphi$	angle between the wire- and rolling axes;
$O_w$	ovalization of wire;
$\alpha$	netting cell angle;
$A_w$	part of the composite cross-section filled by the wires after rolling;
$\mu_c$	netting cell elongation;
5056-A-90-30	example of experiment code: It means: (5056) the type of the matrix alloy – (A) net type – (90) composite type – (30) nominal reduction at rolling;
$e_b, e_w, e_l$	true logarithmic strain over the height, width and length of the sample, respectively;



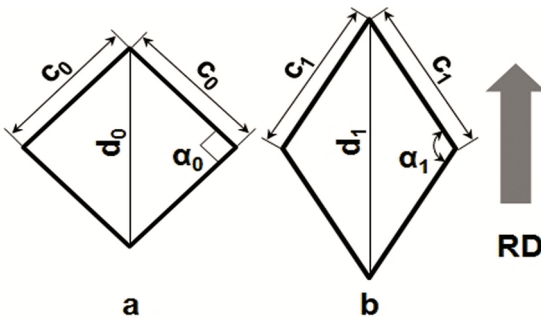


**Figure 3.** Scheme for calculation of the net cell elongation factor for Type 45 composites: a) - net cell before rolling; b) - net cell after rolling;  $c_0$ ,  $d_0$  and  $\alpha_0$  - respectively, initial edge length, diagonal length and cell angle;  $c_1$ ,  $d_1$  and  $\alpha_1$  - respectively, edge length, diagonal length and cell angle after rolling.

clamps equal to 18 mm were sampled from the composite strips for each condition. The tensile tests were carried out on the universal hydraulic testing machine MTS Landmark 250 using a tension speed of 4 mm/min. As a result, the yield strength  $R_{0.2}$ , the tensile strength  $R_m$  as well as two types of elongation at fracture,  $A_{5(Rm)}$  and  $A_5$ , were measured for each specimen.  $A_{5(Rm)}$  - is a calculated value reflecting the sample non-proportional elongation at maximal stress;  $A_5$  - is a measured total sample elongation after the test. For every condition, the mean values of the properties measured from three specimens were taken for further analysis. Images of the samples' length during tension were also taken in equal time intervals using a digital high-speed camera.

### 3. Results

#### 3.1 General results

The delamination of the composites during the rolling wasn't observed for the whole range of experiments. Only composites 6063-0-30 were delaminating during machining of specimens. During the rolling, the wires rather uniformly filled the length and width of the composite strips. No visible breaks or gaps were detected. The chemical removal of one of the matrix layers revealed that the net cells inside the composite were unevenly deformed (See Fig. 4). Thus for the Type 90 reinforcement, the visible substantial bending of transversal wires in the central part of the composite, as well as uneven increase in the distance between them was noticed. (Fig. 4a). The analysis of the transversal wire distortion showed that the thicker "A"-netting is more inclined to bending than the thinner-wire "B"-netting.

At the same time, rolling composites with AW-5056 matrix at a temperature of 500°C results in less wire bending than the rolling of composite with AW-6063 matrix at 200°C. The increase of the strain in the investigated range predictably leads to the increased bend in transversal wires. The angle between the wires (See Fig. 4b) in the Type 45 composite

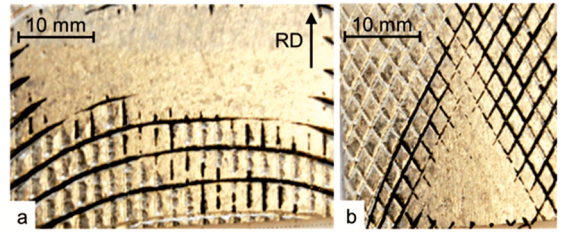


**Figure 4.** Examples of the net distortion in Type 90 (a) and Type 45 (b) composites after rolling: RD - rolling direction.

changed during rolling, but the wire contraction was still less than the Type 90 composite.

As it will be shown below, the true values of the elongation factor for the transversal wires at Type 90 composite are 2...4% lower, while the values of ovalization are overestimated due to the fact that these wires bent during the rolling (See Fig. 4a). Analysis of the net wires intersection area in Type 45 composite (See Fig. 5b) shows that zones of a localized intensive deformation can be detected near these intersections. Their appearance is caused by wire-to-wire compression and by the simultaneous movement of these intersections towards the rolling direction due to the axial tension and elongation of the whole composite.

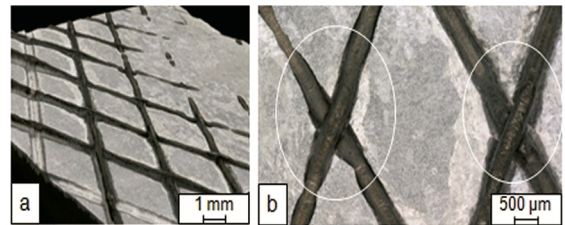


**Figure 5.** Reconstruction of the surface topography, measured by Keyence VHX5000 (a) and the intersections of the net wire (b) inside the rolled Type 45 composite. Marked areas - zones of the localized intensive deformation.

The digital microscope image presented in Fig. 5a is a 3D reconstruction of the net inside the rolled Type 45 composite. Thus, rolling with a 30% nominal reduction, the maximal deviation of the intersection angle  $\alpha_1$  from  $\alpha_0$  in "A"-net was 12° and 13° for composites with AW-5056 and AW-6063 matrices respectively. For the "B"-net, these values were equal to 16° for the both matrix materials. For the composite with AW-6063 matrix, rolled in two passes, the intersection angle  $\alpha$  changed on 32° for the both net types.

#### 3.2 Roll bonding of composites with AW-5056 matrix

The main measured and calculated strain parameters of this roll bonding series are presented in Table 3.

The analysis of the rolling results shows that while straining of transversal wires in the Type 90 composite almost did not occur, the longitudinal wires were intensely strained. The elongation factor of the longitudinal wire  $\mu_{wL}^{90}$

**Table 3.** The strain parameters of rolling composites with AW-5056 matrix.

Experiment code*	$\epsilon_h$	$\epsilon_b$	$\epsilon_l$	$\mu_\Sigma$	$\mu_c$	$\mu_w^{45}$	$\mu_{wL}^{90}$	$\mu_{wQ}^{90}$	$O_w^{45}$	$O_{wL}^{90}$	$O_{wT}^{90}$	$A_w, \%$
5056-A-90-30	-0.32	0.03	0.28	1.28	-	-	1.44	1.08	-	1.13	1.07	2.90
5056-A-45-30	-0.38	0.07	0.34	1.37	1.49	1.36	-	-	1.15	-	-	3.29
5056-B-90-30	-0.37	0.07	0.31	1.35	-	-	1.13	1.02	-	1.1	1.04	1.14
5056-B-45-30	-0.38	0.09	0.33	1.37	1.38	1.21	-	-	1.08	-	-	2.73
5056-0-0-30	-0.37	0.06	0.35	1.35	-	-	-	-	-	-	-	-

which exceeds the elongation factor of the whole composite  $\mu_\Sigma$  indicates additional localized deformation in net knots. In the case where the elongation factor of the longitudinal wires  $\mu_{wL}^{90}$  is considerably smaller than the composite elongation  $\mu_\Sigma$ , such as in specimen 5056-B-90-30, wires breakage inside the composite could be indicated. These assumptions were confirmed by the subsequent sample etching revealing the net structure. This may be caused by the embrittlement of the stainless steel wire during the heating at a temperature of 500 °C.

The smaller values of the wire elongation factor for the Type 45 composite  $\mu_w^{45}$  are compensated for by altering the wire's intersection angle. The angle changed to 12° in the experiment 5056-A-45-30 which, together with the wire elongation factor  $\mu_w^{45} = 1.36$ , enabled net cell elongation factor results of  $\mu_c = 1.49$ . The latter is greater than the elongation factor of the whole composite  $\mu_\Sigma = 1.37$ .

The net cell elongation factor for the experiment 5056-B-45-30  $\mu_c$  was equal to 1.38, which is larger than the elongation factor for the entire composite  $\mu_\Sigma$ . This finding indicates that there is a relatively low probability of wire breakage in this composite. Furthermore, this probability is lower in specimens with a "A"-net, than in those with a "B"-net. Despite the elongation factor of the net cells  $\mu_c = 1.38$  being greater than the total elongation factor of the composite  $\mu_\Sigma = 1.37$ , the wires' fracture during rolling even occurred in the Type 45 composite. However, the development of methods for a quantitative evaluation of wire fracture probability may be the purpose of further research.

Using the same initial roll gap, the lowest reduction was achieved while rolling Type 90 and Type 0 composites. The highest reduction resulted from rolling Type 45 composites. This indicates that the diagonally oriented net promotes the metal flow in the core layer of the composite by reducing internal friction. This effect is greater for the thinner wires ("B"-net). The composite with smaller cells, thinner wires

and a diagonal net orientation also show a greater widening when compared to specimens with a longitudinally oriented "A"-net. However, it should be noted that the widening in this experiment was insignificant.

### 3.3 Single-pass roll bonding of composites with AW-6063 matrix.

The main strain parameters of this rolling series are presented in Table 4.

A more intensive deformation of wires can be seen in this experimental series than with the composites based on AW-5056. Thus, the calculated stretching and ovalization of wires have higher values. In all cases, the elongation factor of wire  $\mu_w$ , including extension of cells in Type 45 composites, was greater than the total elongation factor of the entire composite  $\mu_\Sigma$ . This finding indicates that the wires in the composite were not broken. The larger strain, compared to composites with an AW-5056 matrix, can be explained by the favourable temperature range for the wires deformation. For the wire material, an austenitic stainless steel, the deformation occurs in a range of temperatures around 200 °C, referred to as warm rolling<sup>12</sup>. In Type 45 composites, the cells' diagonal length increased due to the cell transformation from a square form to rhombus. The amounts increased by 1.49 and 1.45 times for the "A"-net and "B"-net respectively. The probability of wire fracture in this case was minimal. Nevertheless, it is important to pay attention to minor differences between part of the "A"-net and "B"-net wires in the cross-sectional area of Type 45 composites.

### 3.4 Two-pass roll bonding of composites with AW-6063 matrix

The rolling was carried out in two passes with 30% of nominal reduction in the first pass and the total nominal

**Table 4.** Strain parameters of rolling composites with AW-6063 matrix with a nominal reduction of 30%\*.

Experiment code	$\epsilon_h$	$\epsilon_b$	$\epsilon_l$	$\mu_\Sigma$	$\mu_c$	$\mu_w^{45}$	$\mu_{wL}^{90}$	$\mu_{wQ}^{90}$	$O_w^{45}$	$O_{wL}^{90}$	$O_{wT}^{90}$	$A_w, \%$
6063-A-90-30	-0.36	0.04	0.32	1.37	-	-	1.68	1.3	-	1.25	1.04	2.51
6063-A-45-30	-0.35	0.05	0.33	1.35	1.49	1.35	-	-	1.11	-	-	4.35
6063-B-90-30	-0.36	0.03	0.34	1.39	-	-	1.24	1.05	-	1.08	1.09	0.91
6063-B-45-30	-0.36	0.04	0.34	1.38	1.45	1.27	-	-	1.1	-	-	3.51



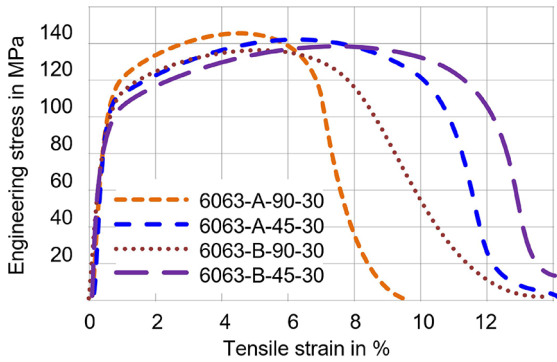


**Figure 8.** Stress-strain curves of composites with AW-6063 matrix.

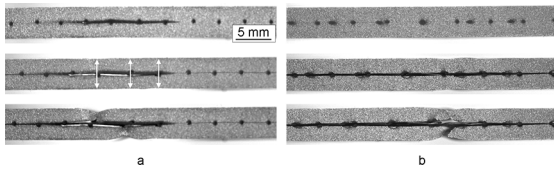


**Figure 9.** The images of the single-pass rolled composite with AW-6063 matrix, made during tensile tests prior to their fracture: a - Type 90, "A"-net (the arrows indicate the necking places of the aluminium matrix); b - Type 45, "A"-net.

Thus, the thinning of the aluminium matrix in Type 90 composite occurs at the location of the transversal wires which serve as stress concentrators, especially after the complete delamination of the composite. In Type 45 composites the role of stress concentrators plays net knots.

### 3.5.3 Two-pass rolled composites with AW-6063 matrix

An analysis of tensile tests results show that all reinforced Type 45 composites, when compared to non-reinforced composites, have slightly higher tensile strength values (See Fig. 10). In terms of reinforcing nets, the comparison of Type 45 composites shows that the composites with "A"-net-reinforcement have higher yield strength, and the ones reinforced with "B"-net have higher ductility values. The strength and ductility of Type 90 composites are 10%-15% and 35%-50% below this level, respectively.

The images captured prior to the fracture of tensile samples (See Fig. 11) show that rolling in two passes provided the solid compound of aluminium matrix layers with a proper bonding between them. There was no significant delamination observed in any test performed.

The main feature of the Type 45 composite, observed at its fracture, is a multiple necking of the sample in the zones between net knots. Due to a strong bonding between the matrix and reinforcing wires, these wires impede strain development. It is also important to note that only a limited delamination in the Type 0 composite was observed, while no delamination was observed in the reinforced Type 45 composite.

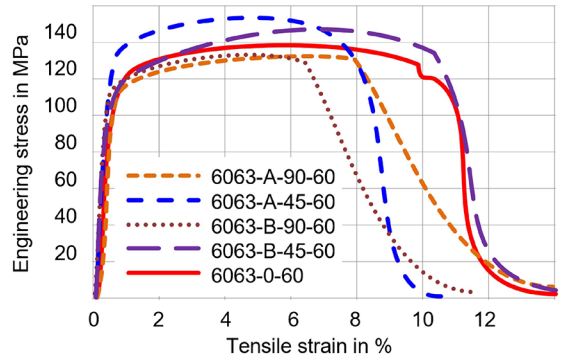


**Figure 10.** Stress-strain curves of composites with AW-6063 matrix rolled in two passes

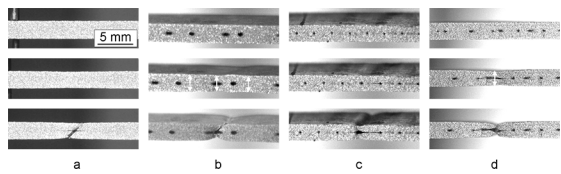


**Figure 11.** Images of two-pass rolled composites with an AW-6063 matrix taken during tensile tests prior to the fracture (the arrows indicate the necking places of aluminium matrix): a - Type 0; b - Type 45, "A"-net; c - Type 90, "B"-net, d - Type 45, "B"-net.

## 4. Discussion

The fact that visible delamination after deformation was not observed suggests the possibility of producing the net-reinforced composites with a matrix of the studied alloys by means of roll-bonding at temperatures of 200-500°C, with a total reduction of about 30%.

It was established that the reduction in these roll bonding experiment is limited by the strength of the reinforcing wire.

The error in the determination of the logarithmic strain was 0.04%-4.63%, caused by the unavoidable inaccuracy in the measuring of the composite length after rolling.

The error in the determination of the elongation factor, wire ovalization and change of cross-sectional area is estimated as  $\pm 3\%$ .

For the majority of experiments, stretching was the main type of wire deformation observed. However, a local reduction of the wires' cross sectional area is observed in the knots of their intersection, particularly for the "A"-net. The relation of ovalization (flattening) to the stretching of the wires depends on the parameters of the deformation zone at rolling. In particular, it depends on the reduction and rolls diameter. The application of netting without intersecting knots can be a purpose for further research.

The "A"-net was most intensely deformed in the Type 45 composite. To avoid wire fracture in this type of composite, the elongation factor of cell diagonal  $\mu_c$  should be directly correlated with a total elongation factor of the composite  $\mu_x$ . If the total elongation factor of the composite  $\mu_x$  is higher than the elongation factor of cell diagonal  $\mu_c$ , then there is a high probability of wire fracture. Furthermore, even if the

elongation factor of cell diagonal  $\mu_c$  is the same or slightly higher than composite  $\mu_c$ , the probability of breakage remains. The balance of these factors requires further clarification. The probability of wire fracture can be estimated as the correlation of the elongation factors of composite and wires, considering a maximum possible elongation for the material of current wire.

Longitudinal wires assume the main deformation in the Type 90 composite. The elongation factor of wire  $\mu_{wL}^{90}$  should be directly correlated with the elongation factor of the composite  $\mu_c$  to predict the possible fracture of these wires.

In the "A"-net, the strain of longitudinal wires of the Type 90 composite is 29%-33% higher than the strain of transversal wires, and does not depend on the matrix material and reduction in the conducted experiments. This difference is about 10%-60% for the "B"-net.

Wire ovalization largely depends on reduction at roll bonding. The ovalization of transversal wires in the Type 90 composite is minimal; a moderate ovalization was observed in the wires of Type 45 composite; and the maximum of this criterion was reached by the longitudinal wires in Type 90 composite.

Deformation of transversal wires in the Type 90 composite occurs mainly due to bending in the rolling direction. The ovalization of transversal wires was negligible for the majority of experiments.

The Type 90 composite showed unsatisfactory results at the tensile tests. It could be related to the exhaustion of plastic properties of the longitudinal wires at rolling, and also to the fact that transversal wires serve as stress concentrators under the tension.

Type 45 composite showed the best results in the tensile tests due to the low stretching of wires at rolling.

Comparison of obtained results with calculated theoretical strength value for reinforced composites shows that the latter was reached only once. The single composite showing so high performance was 5056-A-45-30. The theoretical strength was calculated proportionally to the part of composite cross-section filled by the wires ( $A_w$ ) taking into account estimated tensile strength of wire equal to 900 N/mm<sup>2</sup> using the formula described in<sup>13</sup>:

$$\sigma_{fm} = (\eta) \sigma_f \frac{V_f}{V_{fm}} + \sigma_m \left(1 - \frac{V_f}{V_{fm}}\right) \quad (7)$$

where, according to<sup>13</sup>:  $\sigma_{fm}$  - ultimate tensile stress of the composite;  $\eta$  - reduction factor being existing in range 1-0,5;  $\sigma_f$  - ultimate tensile stress of reinforcement;  $V_f$  - volume of reinforcement inside the composite;  $V_{fm}$  - volume of composite;  $\sigma_m$  - ultimate tensile stress of matrix.

In this study formula (7) was implemented under following conditions: reduction factor  $\eta$  equals to 1;  $\sigma_f = 900$  N/mm<sup>2</sup>; instead the volumetric ratio  $\frac{V_f}{V_{fm}}$  was applied surface  $A_w$ ; as the ultimate tensile stress of matrix was used ( $R_m$ ) value of not reinforced composite from each experiment

(Type 0 composite). Composites rolled at 200°C with reduction 30% were not considered during the evaluation of theoretical strength, due to their 6063-0-30 delamination during machining of specimens.

Due to the small wire diameter, only the Ultimate Tensile Strength (UTS) was taken into account according to the ASTM A 478. It's initial value equals to 630 MPa. Stipulated by the Standard Specification the elongation measurement in 254 mm base weren't performed in this study. The expected UTS value of deformed inside the composite wire, corresponding to 30% strain hardening, is 900 MPa for rolling temperature 500°C. Tensile test of the net's wires wasn't performed after rolling. In the whole experimental procedure the most dangerous for steel 1.4301 is relative long (more than 3 minutes) soaking at a temperature higher than 450°C due to the Chromium carbides formation.

In Fig. 12 the chart showing the ratio of obtained strength ( $R_m$ ) to theoretical ( $R_{m(T)}$ ) strength of rolled composites is presented. The reasons for not reaching of the theoretical values during the experimental investigations seem like a chain of following fails: stress concentration in the net knots as well as near transversal wires; delamination; premature breakage of wires and split of matrix with reinforcement due it's geometrical distortion.

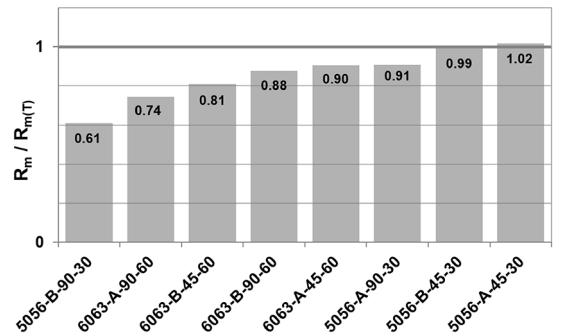


**Figure 12.** Ratio of obtained strength ( $R_m$ ) to theoretical ( $R_{m(T)}$ ) strength of rolled composites.

Wire fracture at rolling reduces the mechanical properties of the whole composite. However, in some cases, it also improves mechanical properties when compared to non-reinforced composites. This suggests that composite strengthening results from the net-reinforcement as well as from the local hardening of the aluminium matrix induced by wires.

Depending on the wire distribution in the composite cross-section and on the bonding strength in matrix-matrix and matrix-reinforcement interfaces, the fracture of composite occurs by the following mechanisms:

- **Delamination → Fracture of layers (D-F).** This mechanism occurs when the composite has a low bonding strength in a matrix-matrix system, and also a relatively small part of wires in the cross section of the composite (Fig. 13);

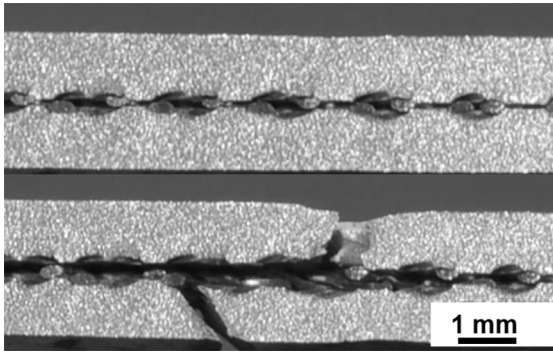


Figure 13. Example of "D-F" mechanism at composite's tension.

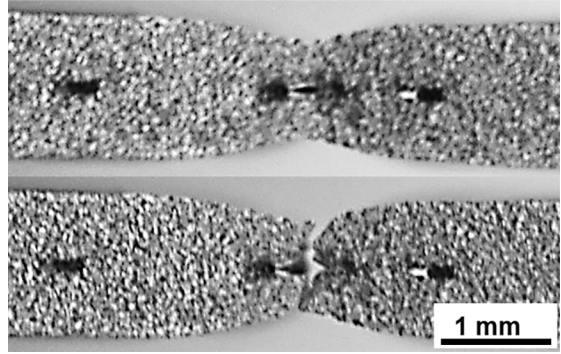


Figure 15. Example of "F" mechanism at composite's tension.

- **Fracture of the first layer → Limited delamination → Fracture of the second layer (F1-D-F2).** This mechanism is characteristic of the composite, in which the part of transversal wires (relative to the tension axis) is small and the bonding strength between matrix and reinforcement is higher than that between the matrix layers. In this case, at the elastic return of the destroyed first layer, the reinforcement "splits" the composite layers (Fig. 14).

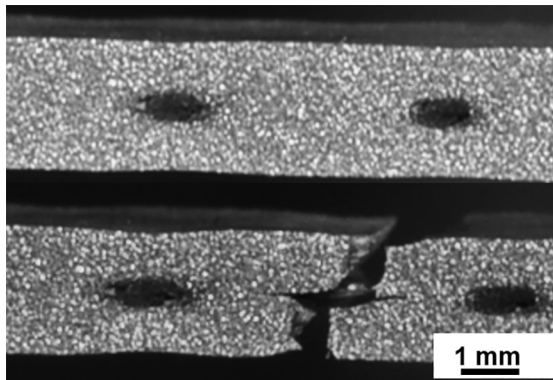


Figure 14. Example of "F1-D-F2" mechanism at composite's tension.

- **Fracture without delamination (F).** This mechanism is characteristic to the composite with a high bonding strength in a matrix-matrix and matrix-reinforcement interfaces as well as with a large part of wires in the cross section (Fig. 15).

These three main mechanisms change each other within development of rolling stresses.

There were no clear evidences of intermetallic phase's presence found during light microscopy investigations. Majority of pictures show little gaps, appeared between the matrix and wire. Metallurgical bonding wasn't expected in such type of reinforcing. It's caused due to the different values of thermal expansion coefficient: for austenitic steel it equals to  $16...18 \cdot 10^{-6} \text{K}^{-1}$ , for the Al-based matrix -  $23...25$

$10^{-6} \text{K}^{-1}$ . In our case the closest contact between the matrix and reinforcement was reached at the rolling temperature. Then, during the further cooling the matrix contracts itself faster than the reinforcement. Therefore, this difference in contraction induces tensile stresses on aluminium-steel phases interface. It means that there are no favorable conditions for the growth of intermetallic phases. That effect was accelerating with a significant heat flow to the rolls during rolling. Probably, the heat treatment after intensive reduction could inspire the growth of intermetallic phases.

## 5. Conclusions and outlook

Improving properties of net-reinforced composites is limited due to an accumulation of tensile strain on wires while rolling. Consequently, when combined with an additional localized intensive compression on the net knots, this effect leads to wire fracture and to an induced longitudinal tensile stress on the entire composite. Thus, there is a contradiction between the strain required for proper bonding of matrix layers (at a given temperature) and stress, induced by that strain, which causes excessive tension on reinforcement wires. The most favorable results in the longitudinal tensile tests were obtained using specimens with a reinforcing net placed diagonally to the rolling axis. On our opinion, a longitudinal orientation of wires is useless and a transversal orientation is dangerous due to the concentration of stress. Parameters of the deformation zone while rolling play a significant role in the distortion of wires inside the composite. The three types of composite fracture were detected. Each of them depends on own composition of followed factors: the part of wires in a cross section of the composite, properties of the wires, orientation of the wires to the rolling axis, 4) properties of the matrix, 5) bonding strength on the net-matrix and matrix-matrix interfaces. Shorter way to improvement of the composite's tensile properties is not to use net reinforcements. From other hand improvement also could be reached with increment of wires part in the composite's cross section. However, it leads to the growth

of specific weight. Unattended, in case of usage of net, it could be net with minimized knees at wire intersections.

## 6. Acknowledgements

The investigative results presented in the work were obtained with support from the German Academic Exchange CNPQ (n 124566) Service (DAAD) in the scope of the cooperative German-Ukrainian exchange project "Praxispartnerschaft Metallurgie".

## 7. Funding Acknowledgements

The German Academic Exchange Service (DAAD) in the scope of the cooperative German-Ukrainian exchange project "Praxispartnerschaft Metallurgie" supported this work.

## 8. References

1. Portnoi KI, Salibekov SE, Svetlov IM, Chubarov VM. *Struktura I svoystva kompozitsionnich materialov (Structure and properties of composite materials)*. Moscow: Mashinostroenie; 1979.
2. Forsyth PJ, George RW, Ryder DA, Vian RE, inventors; National Research Development Corporation, assignee. *Composite metal structural components*. United States patent US 3314825. 1967 Apr 18.
3. Gotoh K, inventor; Takeo Kagitani, assignee. *Process for making steel-reinforced aluminum members*. United States patent US 3201862 A. 1965 Aug 24.
4. Cole DQ, Davis LRW, Sumner EV, inventors. Harvey Aluminum, Incorporated Application, assignee. *Process for the production of aluminum-steel composite*. United States patent US 3551996 A. 1971 Jan 5.
5. Haga T, Takahashi K, Nakamura R, Watari H. Roll Casting of Net Inserted Aluminum Alloy Strip. *International Journal of Material Forming*. 2010;3(Suppl 1):1063-1066.
6. Grydin O, Stolbchenko M, Schaper M. Twin-Roll Casting of Carbon Fiber-Reinforced and Glass Fiber-Reinforced Aluminum Strips. In: Williams E, ed. *Light Metals 2016*. Hoboken: John Wiley & Sons; 2016.
7. Grydin O, Gerstein G, Nürnberger F, Schaper M, Danchenko V. Twin-roll casting of aluminum-steel clad strips. *Journal of Manufacturing Processes*. 2013;15(4):501-507. DOI: 10.1016/j.jmapro.2013.08.008
8. Stolbchenko M, Grydin O, Nürnberger F, Samsonenko A, Schaper M. Sandwich Rolling of Twin-roll Cast Aluminium-steel Clad Strips. *Procedia Engineering*. 2014;81:1541-1546. DOI: 10.1016/j.proeng.2014.10.187
9. Manesh HD, Shahabi HS. Effective parameters on bonding strength of roll bonded Al/St/Al multilayer strips. *Journal of Alloys and Compounds*. 2009;476(1-2):292-299.
10. Haga T, Takahashi K, Nakamura R, Kumai S. Casting of wire-inserted composite aluminum alloy strip using a twin roll caster. *Journal of Materials Processing Technology*. 2007;192-193:108-113.
11. Haga T, Takahashi K, Kumai S, Warari H. Casting of a wire inserted strip using a twin roll caster equipped with two nozzles. *Advanced Materials Research*. 2011;337:556-559.
12. Frolov YV, Mamuzic I, Danchenko VN. The heat conditions of the pilger rolling. *Metallurgia*. 2006;45(3):179-184.
13. Heinrich W, Nixdorf J. Die Faser- und Fadenverstärkung von plastischen und spröden Matrixmaterialien. *Materialwissenschaft und Werkstofftechnik*. 1972;3(1):21-26.